Published in final edited form as:
Circ Res. 2010 July 23; 107(2): 294–304. doi:10.1161/CIRCRESAHA.110.223172.

Myocardin-related transcription factor-A controls myofibroblast activation and fibrosis in response to myocardial infarction

Eric M. Small[1], **Jeffrey E. Thatcher**[2], **Lillian B. Sutherland**[1], **Hideyuki Kinoshita**[5], **Robert D. Gerard**[1,3], **James A. Richardson**[1,4], **J. Michael DiMaio**[2], **Hesham Sadek**[3], **Koichiro Kuwahara**[5], and **Eric N. Olson**[1]

[1] Department of Molecular Biology, University of Texas Southwestern Medical Center, Dallas, Texas, USA

[2] Department of Cardiovascular and Thoracic Surgery, University of Texas Southwestern Medical Center, Dallas, Texas, USA

[3] Department of Internal Medicine, University of Texas Southwestern Medical Center, Dallas, Texas, USA

[4] Department of Pathology, University of Texas Southwestern Medical Center, Dallas, Texas, USA

[5] Department of Medicine and Clinical Science Kyoto Graduate School of Medicine, Kyoto, Japan

Abstract

Rationale—Myocardial infarction (MI) results in loss of cardiac myocytes in the ischemic zone of the heart followed by fibrosis and scar formation, which diminish cardiac contractility and impede angiogenesis and repair. Myofibroblasts, a specialized cell type that switches from a fibroblast-like state to a contractile, smooth muscle-like state, are believed to be primarily responsible for fibrosis of the injured heart and other tissues, although the transcriptional mediators of fibrosis and myofibroblast activation remain poorly defined. Myocardin-related transcription factors (MRTFs) are SRF co-factors that promote a smooth muscle phenotype and are emerging as components of stress-responsive signaling.

Objective—We aimed to examine the effect of MRTF-A on cardiac remodeling and fibrosis.

Methods and Results—Here we show that MRTF-A controls the expression of a fibrotic gene program that includes genes involved in extracellular matrix production and smooth muscle cell differentiation in the heart. In MRTF-A null mice, fibrosis and scar formation following MI or Angiotensin (Ang) II treatment are dramatically diminished compared with wild-type littermates. This protective effect of MRTF-A deletion is associated with a reduction in expression of fibrosis-associated genes, including *collagen 1a2*, a direct transcriptional target of SRF/MRTF-A.

Conclusions—We conclude that MRTF-A regulates myofibroblast activation and fibrosis in response to the renin-angiotensin system and post-MI remodeling.

Keywords

MRTF-A; myocardial infarction; fibrosis; collagen; myofibroblast; transcription

Author for correspondence: Eric N. Olson, Department of Molecular Biology, 5323 Harry Hines Blvd. Dallas, Texas, 75390-9148, USA. Phone: 214-648-1187, Fax: 214-648-1196, eric.olson@utsouthwestern.edu.

Disclosures: none

Myocardial infarction (MI) results in death of ischemic cardiac tissue followed by an inflammatory response and replacement of contractile tissue with a fibrotic scar 1. Scar formation in response to MI is largely mediated by myofibroblasts, a unique, contractile cell type that displays features of both fibroblasts and smooth muscle cells (SMCs) 2. Extracellular signals, mechanical force, or tissue injury trigger myofibroblast activation and the production of smooth muscle α actin (SMA)-containing stress fibers, which contribute to the force generation and retraction required for wound healing 2–6. Myofibroblasts also secrete extracellular matrix (ECM) components, including collagen 1a1 (Col1a1), collagen 1a2 (Col1a2), collagen 3a1 (Col3a1), and matrix metalloproteases, which result in the formation of granulation tissue and a fibrotic scar 2, 7.

Serum response factor (SRF) plays a primary role in the regulation of nearly every known smooth muscle-specific gene via binding to the sequence [$CC(A/T)_6GG$], termed a CArG box or serum response element (SRE) 8, 9. The transcriptional activity of SRF is enhanced through its association with the co-activators myocardin and the myocardin-related transcription factors (MRTF-A/MAL/MKL1 and MRTF-B/MKL2) 8, 10–12. Myocardin is restricted to cardiac and smooth muscle and is required and sufficient with SRF for the activation of smooth muscle gene expression 10, 13–16. MRTF-A and MRTF-B are broadly expressed and are regulated at the level of sub-cellular distribution via interactions with the actin cytoskeleton 11, 17–19. MRTF-A and MRTF-B possess a unique N-terminal RPEL domain that mediates binding to G-actin and cytoplasmic sequestration 20. Stress signals, mechanical force, and changes in cell shape result in the activation of Rho – Rho kinase (ROCK) signaling, reorganization of the actin cytoskeleton and nuclear translocation of MRTF-A, thereby linking actin dynamics to SRF-dependent gene transcription 17, 21–26.

ROCK-dependent signaling enhances the transcription of genes encoding ECM components and SMA by myofibroblast-like cells in models of fibrotic pathology 27–30. ROCK haploinsufficiency or pharmacological inhibition of ROCK reduces cardiac fibrosis in response to MI, ischemia reperfusion or pressure overload 31–35. ROCK activation contributes to the nuclear accumulation of MRTFs and the activation of SMA transcription in vitro 28, 36. An SRF containing complex has been implicated in the induction of a myofibroblast phenotype 37, 38, but whether SRF contributes to fibrosis in vivo is unknown.

In this study, we demonstrate that genetic deletion of MRTF-A in mice results in reduced scar formation following MI or Angiotensin (Ang) II treatment. The diminution of scar formation in MRTF-A null mice following MI is associated with a reduced number of SMA-positive myofibroblasts and diminished expression of fibrosis-associated genes in the border zone (BZ) of the infarct. We identify a set of MRTF-A -regulated genes that encode markers of myofibroblasts and fibrosis, including those encoding smooth muscle sarcomeric and structural proteins, and ECM components. We show that MRTF-A responds to TGFβ-1 in cardiac fibroblasts (CFs) and contributes to the induction of a collagen-secreting SMA-enriched myofibroblast-like phenotype by directly activating the *Col1a2* promoter via a conserved CArG element. These results reveal MRTF-A as a key regulator of cardiac remodeling and provide insight into the mechanism whereby ROCK inhibition reduces pathological fibrosis.

Methods

Cell culture and transfection

10T1/2 cells were grown in MEM Eagles medium in 6-well plates and transiently transfected with 500 ng of empty pcDNA3.1 control or pcDNA3.1-MRTF-A plasmid for 48hrs prior to RNA isolation. CFs grown in DMEM were treated as noted in text for 24–48

hrs followed by RNA or protein isolation. CF proliferation was determined with the CellTiter 96 Aqueous One Solution Cell Proliferation Assay (Promega) using the manufacturer's protocol.

For luciferase assays, CFs or COS cultured in 24 well plates were transfected with a total of 300ng of plasmid DNA using FuGENE6 (Roche). 20ng of pCMV-lacZ was used as an internal control and total plasmid amount was kept constant using empty pcDNA3.1. 48 hrs after transfection luciferase and β-galactosidase assays were carried using a luciferase assay kit (Promega).

Col1a2 reporter construction

420 bp of the mouse *Col1a2* promoter was amplified using high fidelity Taq polymerase (TAKARA) and the following oligonucleotides containing 5′ KpnI and 3′ XhoI linkers: Col1a2 For: 5′ – GGTACCGACAGCTCCTGCCTTTTCATC –3′; Col1a2 Rev: 5′ – CTCGAGTAAAATAATAAAGCCCAGACC – 3′. The resulting PCR product was cloned into the KpnI and XhoI sites of the pGL3-basic luciferase vector (Invitrogen). Mutation of the CArG element was accomplished using the QuickChangeII site directed mutagenesis kit and the manufacturer's protocol (Stratagene). The oligonucleotides used for PCR amplification are as follows: Col1a2 mutCArG For: 5′ – CCTAAAGTGCTTACACACGTGGCAAGGGCG – 3′; and Col1a2 mutCArG Rev: 5′ – CGCCCTTGCCACGTGTGTAAGCACTTTAGG – 3′. All constructs were sequence verified.

Immunocytochemistry

CFs were infected with a flag-tagged MRTF-A adenovirus at an MOI of 10 and were treated with TGFβ-1 (10 ng/ml) and/or Y-27632 (10 μM) 24 hrs prior to fixation with cold methanol. Indirect immunofluorescence was performed with a mouse monoclonal Flag M2 antibody (Sigma) or Cy3-conjugated anti-SMA antibody (Sigma, clone 1A4, 1:200). Confocal images were captured using a Zeiss LSM-510 microscope.

Western blot

Antibodies directed against SMA (Sigma), SM22 (Abcam), Collagen I (Abcam), and tubulin (Sigma) were used to determine protein levels by Western blot. Non-denaturing PAGE was performed to detect Collagen I protein by Western blot.

Histology and immunohistochemistry

Tissues were fixed in 4% paraformaldehyde, embedded in paraffin, and sectioned at 5-μm intervals. Hematoxylin and eosin and Masson's Trichrome staining were performed using standard procedures. SMA staining was performed on paraffin embedded sections using a Cy3-conjugated anti-SMA antibody (Sigma, clone 1A4, 1:200). Nuclei were visualized using Dapi in vectashield mounting medium (Vector laboratories). SMA positive vessels and myofibroblasts were counted in the BZ of three WT and three MRTF-$A^{-/-}$ animals and represented as the average +/− SEM. Proliferation and cell death was detected using a phospho-Histone-H3 antibody or the In situ cell death detection kit (Roche) and manufacturer's protocol, respectively.

RNA analyses

Total RNA was isolated using Trizol reagent (Invitrogen) according to manufacturer's protocol. 2 μg of RNA was used to generate cDNA using Superscript III (Invitrogen) following manufacturer's protocol and detected using Taqman primer and probesets.

Collagen Synthesis Assay

[^{3}H]-Proline incorporation was performed to determine the effects of MRTF-A over-expression on collagen synthesis. CFs at passage 2 or 3 were cultured in 24-well tissue culture dishes for 48hrs, or until confluent, in DMEM supplemented with 10% FBS under standard culture conditions. CFs were then made quiescent by serum starvation for 24 hrs, infected with 10MOI of adenovirus mediating the expression of MRTF-A or control β-galactosidase, and cultured in SF conditions for an additional 24 hrs. CFs were then stimulated with the addition of 2.5% FBS, TGFβ-1 (10 ng/ml), Y-27632 (10 μM), or a combination of TGFβ-1and Y-27632 for 48hrs in the presence of [^{3}H]-Proline (1 μCi/ml, PerkinElmer Life Sciences). CFs were then washed three times with Dulbelcco's PBS and protein was precipitated with ice cold 5% TCA for 1hr. The precipitate was then solubilized with 400 μl of 0.2 M NaOH at 37°C for 30 min. Radioactivity was determined by liquid scintillation counting. Each condition was performed in quadruplicate and repeated in 3 independent experiments.

Chromatin immunoprecipitation assay

Chromatin immunoprecipitation was performed using the EZ-ChIP kit (Millipore) using manufacturer's instructions. Briefly, native chromatin from 10T1/2 was crosslinked and immunoprecipitated with antibodies directed against SRF (Santa Cruz), RNA PolII (Millipore), or mouse IgG (Millipore). Col1a2 promoter sequences or GAPDH was detected using PCR amplification. Chromatin was incubated with 2 μg of an immunoprecipitating antibody against endogenous SRF (Santa Cruz), RNA PolII (Millipore), or mouse IgG (Millipore), followed by immunoprecipitation with Protein G beads (Millipore) overnight at 4°C.

Electrophoretic Mobility Shift Assay

EMSA was performed using double stranded oligonucleotides corresponding to the Col1a2 CArG sequence. 4 μl of protein lysate from flag-SRF or empty pcDNA3.1 transfected COS cells was incubated with ^{32}P-labeled oligonucleotide probes in the presence of 1 μl of poly dIdC (1.0 μg/μl) for 20 min. at room temperature. Supershift formation was detected by adding 2μl anti-Flag M2 antibody (Sigma).

Myocardial infarction

Myocardial infarctions were generated using male MRTF-A$^{-/-}$ and WT mice at 12 weeks of age (25–30g) by surgical ligation of the left anterior descending (LAD) coronary artery. Sham operated mice underwent the same procedure without occlusion of the LAD. For determination of infarct size, at least four images of Trichrome stained sections per heart were imported to OpenLab 3.1 and the area of Trichrome staining was measured and taken as a percentage of the total LV area in each section. For the studies designed to measure AAR for infarct, 0.3% methylene blue dye was perfused throughout the animal using direct LV administration immediately following confirmation of myocardial ischemia. Perfusion was carried out until significant staining of cardiac tissue had occurred and no further increase in stained area was apparent for 1 minute. The mouse was then further perfused with 4% paraformaldehyde in saline in order to ensure the proper fixation of tissue and vital dye. The heart was then collected and analyzed for AAR. The heart was photographed in whole mount to document the size of stained (perfused) versus unstained (unperfused) regions. The heart was then histologically dissecting into 3 equal size transverse sections, starting at the site of ligature and progressing towards the apex of the heart. Stained LV tissue was separated from unstained tissue, and weighed. The proportion of unstained versus stained tissue based on dry weight determined the AAR.

Angiotensin II infusion

Ang II (dissolved in 0.01 mol/l acetic acid) was subcutaneously infused at the rate of 0.6 mg/kg/day for 2 weeks using an osmotic minipump (Alzet model 2002; URECT Corp., Cupertino, USA) implanted in each mouse. After 2 weeks Angiotensin II infusion, left ventricles were then fixed in 10% formaldehyde. To determine the extent of collagen fiber accumulation, we randomly selected fields and measured the Masson's Trichrom stained interstitial fibrosis area in relation to the total left ventricular area using microscopy BIOREVO BZ-9000 (Keyence, Osaka, Japan). Perivascular fibrosis area was excluded in the present study.

Data and statistical analysis

Results are presented as mean +/− SEM unless otherwise stated. Statistical analysis of group differences was performed by Student's two-tailed t-test with unequal variance and significance between groups of FS% was performed using multiple measures two-factor ANOVA. Significance was considered as $P < 0.05$.

Mouse mutants and animal care

All experiments utilizing animals were previously approved by the Institutional Animal Care and Use Committee at UT Southwestern Medical Center. The MRTF-A$^{-/-}$ mouse line used in this study has been previously reported 19. Mice were genotyped using previously described PCR strategies.

Results

MRTF-A$^{-/-}$ mice display reduced cardiac fibrosis after MI

ROCK signaling has been implicated in myofibroblast activation in diseases associated with excessive fibrosis, including cardiac remodeling following MI 32, 33. In light of the role of MRTF-A as a mediator of ROCK signaling and stress-dependent gene expression in cultured cells 21, 22, we investigated the potential involvement of MRTF-A in the response of the heart to MI, by surgical ligation of the left anterior descending coronary artery in wild type (WT) and MRTF-A$^{-/-}$mice. Two weeks following ligation, WT mice developed an extensive fibrotic scar that spanned the majority of the left ventricular free wall (Fig. 1A-a1, a2), as visualized grossly and by Masson's trichrome staining of histological sections. The infarcted region typically displayed significant thinning and dilatation in association with fibrosis. In contrast, we observed a pronounced reduction in infarct size in MRTF-A$^{-/-}$ hearts as assessed by the size of the fibrotic scar (Fig. 1A-b1, b2). MRTF-A deletion resulted in an ~50% reduction in scar size, as quantified by trichrome staining/LV ratio (Fig. 1B). Post-MI lethality was nearly identical between WT and MRTF-A$^{-/-}$ mice (data not shown) implying adequate initial scar formation to allow wound healing and prevent cardiac rupture. Assessment of cardiac function at baseline and at 3, 7 and 14 days post-MI revealed that although MRTF-A$^{-/-}$ mice tended towards improved fractional shortening (FS%) compared to WT mice, this improvement did not reach statistical significance (Online Figure I).

The reduction of infarct size in MRTF-A$^{-/-}$ mice could, in principal, result from a reduced propensity to generate an infarct or an increased capacity for healing and regeneration of healthy cardiac tissue. To address these possibilities, we first determined the size of the area at risk (AAR) for infarction in WT and MRTF-A$^{-/-}$ mice by perfusing animals with methylene blue. Gross examination of hearts immediately after ligation revealed a similar area of perfusion in WT and MRTF-A$^{-/-}$ mice (Fig. 1C). Quantification of the mass of non-perfused versus perfused myocardial tissue confirmed that deletion of MRTF-A did not result in a reduction of the AAR (Fig. 1D). The AAR was also not altered in MRTF-A$^{-/-}$

mice 24 hours post-MI (Fig. 1D). These results suggest the collateral vessel architecture is not significantly affected by the absence of MRTF-A.

We next determined whether MRTF-A deletion affected cell death in the infarct zone 24 hours post-MI. Staining of histological sections for TUNEL revealed significant cell death throughout the infarcted region, although the percentage of TUNEL positive nuclei was nearly identical between WT and MRTF-A$^{-/-}$ animals (Fig. 1E and Online Figure II). Finally, to examine the possibility that hearts of MRTF-A$^{-/-}$ mice might display increased propensity towards regeneration, we determined whether MRTF-A$^{-/-}$ CMCs underwent re-entry into the cell cycle. Immunostaining of hearts from WT or MRTF-A$^{-/-}$ mice 14 days post-MI for phospho-histone H3 and the CMC marker α-actinin did not reveal a significant alteration in proliferating CMCs (Fig. 1F and Online Figure III). There was however a trend towards decreased proliferation of non-CMCs in the hearts of MRTF-A$^{-/-}$ animals (Fig. 1F and Online Figure III). We conclude that reduced infarct size observed in MRTF-A$^{-/-}$ mice is not a consequence of alterations in AAR, cell viability, or regenerative capacity, and may reflect a direct role in remodeling and scar formation.

MRTF-A regulates collagen expression post-MI

We isolated tissue from the infarct border zone (BZ) and remote healthy tissue 14 days post-MI for quantitative Real-Time PCR. Sham-operated mice were used as controls. Multiple markers of the ECM and fibrotic remodeling were elevated in the BZ of WT animals, as expected (Fig. 2). Up-regulation of Col1a1, Col1a2, Col3a1, and elastin (Eln), in the BZ of wild type mice, was attenuated in the BZ of MRTF-A$^{-/-}$ mice as demonstrated by Real-Time RT-PCR (Fig. 2A). The pronounced diminution of these markers in MRTF-A$^{-/-}$ mice (Fig. 2A) is consistent with the reduced injury in these animals (Fig. 1A and B). The reduction of fibrosis following MI was not accompanied by a significantly diminished expression of TGFβ-1, -2, and -3 in the BZ suggesting normal cytokine activation (Fig. 2B). Expression of atrial natriuretic factor (ANF) was reduced in the BZ of MRTF-A$^{-/-}$ mice, further indicating a decrease of pathological remodeling (Fig. 2C) although Tenascin C (TnC), a marker of cardiac repair after MI, was similarly induced in the BZ of WT and MRTF-A$^{-/-}$ mice (Fig. 2C). The close correlation between the induction of collagen gene expression following MI and MRTF-A genotype implicates MRTF-A in the promotion of scar formation following MI.

MRTF-A regulates myofibroblast expression of SMC markers following MI

Since the myofibroblast is a primary contributor to ECM deposition and scar formation following MI 1, we examined the expression of smooth muscle markers of myofibroblast activation in 14-day post-MI hearts. Expression of SM22 and SMA was attenuated in the BZ and remote tissue of MRTF-A$^{-/-}$ animals 14-days post-MI, as assessed by quantitative RT-PCR (Fig. 3A). We next determined the localization of SMA in WT and MRTF-A$^{-/-}$ hearts 14 days after MI by immunohistochemistry (Fig. 3B). Immunostaining of histological sections for SMA revealed that the BZ of WT mice contained numerous spindle-shaped SMA-positive cells, or aggregates of SMA-positive cells not associated with a vessel, which are indicative of myofibroblast-like cells (Fig. 3B-a"). In contrast, the BZ of MRTF-A$^{-/-}$ mice possessed significantly fewer SMA-positive myofibroblasts than WT animals (Fig. 3B-b"). Quantification of SMA-positive myofibroblasts in the BZ demonstrated a higher density (~3-fold) in WT than in MRTF-A$^{-/-}$ animals (Fig. 3C). SMA is also highly expressed in arterioles that infiltrate the BZ of the infarct. Quantification of the number of SMA positive arterioles in the BZ of WT and MRTF-A$^{-/-}$ hearts revealed a slight, but insignificant increase in the number of arterioles in MRTF-A$^{-/-}$ animals (Fig. 3D).

MRTF-A$^{-/-}$ mice display reduced fibrosis in response to AngII

Since MRTF-A$^{-/-}$ mice are protected from excessive scar formation following MI, and the renin-angiotensin system is a major mediator of post-MI fibrosis, we asked whether MRTF-A also played a role in AngII-mediated fibrosis. Following 14 days of AngII infusion (0.6 mg/kg/day), WT mice displayed profound interstitial fibrosis, as assessed by Masson's trichrome staining of histological sections through the LV (Fig. 4A). In contrast, MRTF-A$^{-/-}$ littermates were protected from fibrosis in response to AngII infusion (Fig. 4A).

Quantification of the percent LV area stained for Masson's trichrome following AngII treatment revealed a nearly complete protection from fibrosis upon MRTF-A deletion (Fig. 4B). Quantification of the expression of collagen genes after 14 days of AngII treatment revealed enrichment of Col1a2 and Col3a1 expression in AngII treated WT mice, which was significantly attenuated in MRTF-A$^{-/-}$ mice (Fig. 4C), confirming the reduction of fibrosis observed in these animals. Likewise, the stimulation of SMA and SM22 expression seen in WT animals was not observed in MRTF-A$^{-/-}$ mice (Fig. 4C). These results further suggest a role for MRTF-A in promoting a myofibroblast phenotype and fibrotic remodeling in the heart.

Regulation of a myofibroblast phenotype by MRTF-A

To test whether MRTF-A was sufficient to induce myofibroblast-associated genes that were down-regulated in MRTF-A$^{-/-}$ mice, we enforced the expression of MRTF-A in cultured primary ventricular neonatal CFs by adenoviral-mediated expression. In contrast to myocardin, which is specifically expressed in the CMCs of the heart, MRTF-A is expressed in both CMCs and CFs (Fig. 5A). As shown in Figure 5, over-expression of MRTF-A in CFs resulted in a dramatic increase in the expression of SMA and SM22 (Fig. 5B). Immunocytochemical detection of SMA in cultured CFs confirmed the enrichment of SMA by MRTF-A, compared with β-gal infected CFs (Fig. 5C). MRTF-A over-expression in CFs resulted in the accumulation of SMA into highly organized stress fibers, a hallmark of myofibroblast activation, in contrast to being primarily localized to cortical actin in control cells (Fig. 5C).

TGFβ-1 promotes the nuclear translocation of MRTF-A in a ROCK dependent manner

TGFβ-1 promotes a contractile myofibroblast phenotype in multiple organs including the heart, kidneys, liver, and skin. TGFβ-1 induced a robust elevation in SMA immunostaining in CFs, which was localized primarily to stress fibers (Fig. 6A). The ROCK inhibitor Y-27632 largely blocked the induction of SMA by TGFβ-1 and MRTF-A, while modestly inhibiting SMA staining at baseline (Fig. 6A). Because MRTF-A undergoes nuclear translocation in response to TGFβ-1 and ROCK signaling in kidney epithelial cells 36, 39, we examined whether TGFβ-1 and ROCK could influence the activity of MRTF-A in CFs. MRTF-A displayed predominantly cytoplasmic localization in CFs cultured in serum free media or in the presence of Y-27632 (~10–20% nuclear; Fig. 6B and C). Treatment of CFs with TGFβ-1 resulted in a shift of MRTF-A to the nucleus; the number of cells displaying cytoplasmic restriction of MRTF-A was significantly reduced with a larger proportion displaying nuclear and cytoplasmic staining or nuclear enrichment (~50% nuclear; Fig. 6B and C). Y-27632 partially blunted the nuclear accumulation of MRTF-A in response to TGFβ-1 suggesting TGFβ-1 dependent nuclear translocation is also influenced by ROCK activity (~40% nuclear; Fig. 6B and C).

Col1a2 is a direct target of MRTF-A

Since MRTF-A induced the expression of SMC markers indicative of a myofibroblast phenotype, we next assessed the ability of MRTF-A to influence the deposition of collagen

by CFs, which largely mediate the fibrotic response following MI. We used [^{3}H]-Proline incorporation to quantify collagen synthesis by CFs subjected to various stimuli. Importantly, MRTF-A over-expression did not stimulate CF proliferation (Online Figure IV), consistent with reports implicating SRF and myocardin in promotion of differentiation and inhibition of proliferation in CMCs 40. Treatment of CFs with serum or TGFβ-1 resulted in elevated collagen production (Fig. 7A). MRTF-A over-expression in CFs also resulted in a significant elevation in collagen synthesis, and this increase was further stimulated by serum or TGFβ-1 (Fig. 7A). In contrast, inhibition of Rho signaling with Y-27632 resulted in the diminution of MRTF-A dependent collagen synthesis (Fig. 7A). We also detected increased levels of Col1a2, SMA, and SM22 protein in CFs over-expressing MRTF-A (Online Figure V). Col1a2 mRNA levels were also increased in response to MRTF-A overexpression as revealed by quantitative Real Time RT-PCR (Fig. 7B).

An evolutionarily conserved CArG box exists within the previously characterized Smad3 and Sp1-dependent promoter region of the *Col1a2* gene 41 (Fig. 7C). An antibody directed against the endogenous SRF protein precipitated chromatin containing the *Col1a2* CArG box in a TGFβ-1 independent manner (Fig. 7D). SRF also efficiently bound to the *Col1a2* CArG box in gel mobility shift assays (Fig. 7E). A 420bp *Col1a2* promoter fragment linked to a luciferase reporter was activated in a dose-dependent manner by MRTF-A, and mutation of the CArG box attenuated MRTF-A responsiveness (Fig. 7F). Furthermore, the *Col1a2* promoter displayed a dose-dependent induction by MRTF-A in primary CFs (Fig. 7G), and mutation of the CArG box completely abolished the stimulation of MRTF-A activity by TGF-β-1 (Fig. 7H). We conclude that MRTF-A directly regulates Col1a2 gene expression to promote fibrosis and scar formation following MI.

Discussion

The results of our study reveal a novel role of MRTF-A in promoting a transcriptional response to MI and AngII infusion. We demonstrate that TGFβ-1 and ROCK modulate MRTF-A subcellular localization and activity in CFs, and that MRTF-A induces a subset of genes consistent with a myofibroblast-like cell type, resulting in collagen synthesis in vitro and in vivo (Fig. 8). Furthermore, genetic deletion of MRTF-A in mice abrogates fibrosis in response to MI and leads to a reduction of myofibroblast induction and scar formation. These findings suggest that attenuation of MRTF-A activity may contribute to the therapeutic effect of ROCK inhibition on fibrotic diseases.

Stress-responsive regulation of collagens by MRTF-A

Up-regulation of multiple markers of the ECM, including Col1a1, Col1a2, Col3a1, and elastin, was dramatically attenuated in MRTF-A$^{-/-}$ mice following MI or AngII treatment. We identify the *Col1a2* promoter as a novel target of MRTF-A/SRF. We have also identified an evolutionarily conserved CArG box upstream of the transcriptional start site of the *Col3a1* gene, adjacent to previously characterized regulatory elements 42. These findings suggest a potential role for MRTF-A in the direct regulation of a battery of fibrosis-associated genes in addition to previously defined targets associated with the actin cytoskeleton or smooth muscle sarcomeric organization.

Interestingly, the *Col1a2* promoter contains a conserved CArG box harboring a G/C substitution in the A/T rich core. This type of CArG degeneracy diminishes binding affinity for free SRF, resulting in a low level of basal expression 43. The results of our study support the hypothesis that CArG degeneracy may be important for stress-responsive activation of gene expression upon nuclear accumulation of SRF co-factors such as MRTF-A.

MRTF-A activation and TGFβ-1

TGFβ-1 - Smad signaling is the best-characterized contributor to myofibroblast activation and fibrosis 44⁻47. TGFβ-1 and its transcriptional mediators, Smad2, 3, and 4, are activated following MI 46⁻48. The TGFβ-1-Smad3 pathway is a major mediator of post-MI remodeling, including the induction of SMA and SM22-enriched myofibroblasts and the transition to fibrosis 44, 45. Smad3 null mice display reduced interstitial fibrosis and cardiac remodeling in response to infarction 49, and abnormal TGFβ-1 – Smad – dependent activation of the myofibroblast lineage can lead to excessive fibrosis that results in chronic fibrotic diseases 45, 50. An SRF/myocardin containing complex has been shown to activate the *SM22* promoter following TGFβ-1 stimulation of 10T1/2 cells to myofibroblasts 37. Recent studies have also documented the modulation of MRTF-A sub-cellular localization and activity in response to TGFβ-1 signaling in kidney epithelial cells 36, 39. The results of our study extend these findings and reveal a novel function of MRTF-A in contributing to myofibroblast activation and ECM deposition in response to TGFβ-1 stimulation of CFs.

TGFβ-1 induced myofibroblast activation and fibrosis is blocked by ROCK inhibition in certain contexts, suggesting cooperation between these signaling pathways. Rho-ROCK signaling plays a major role in sensing the environment and generating a cellular response to injury or stress. Mechanical force or receptor-mediated stimulation of the Rho signaling cascade has been shown to activate ROCK and MLC-kinase, promoting a smooth muscle-like myofibroblast phenotype. ROCK and MLC-kinase also stimulates actin cytoskeleton rearrangement, and nuclear translocation of MRTF-A, which contributes to SMC-specific gene expression, thus linking cellular stress to SRF/MRTF-A mediated transcriptional activation 17, 20⁻23. Rho signaling is also involved in pathological fibrosis of multiple tissues 27⁻30, 35. Therefore, it seems reasonable that MRTF-A may contribute to ROCK-mediated myofibroblast activation and fibrotic remodeling.

Recently, myofibroblast activation following ischemia reperfusion and kidney injury has been suggested to originate from circulating inflammatory cells 35, 51, 52. Monocyte/macrophage deletion significantly attenuated kidney fibrosis following unilateral ureteric obstruction 51. Furthermore, bone marrow-derived cells from a donor mouse were detected within the myofibroblast population of the fibrotic heart of host mice, while ROCK-1 null mice displayed attenuation of this fibrotic response 52. While the most straightforward interpretation of our results is that MRTF-A mediates ROCK-1 signaling in cardiac myofibroblasts during cardiac fibrosis following MI and AngII treatment, it is formally possible that another MRTF-A dependent cell population could contribute to this response. It is also possible that MRTF-A activity in CMCs or SMCs may also contribute to the development of fibrosis following MI or AngII administration. Although MRTF-A is robustly expressed in CFs and over-expression of MRTF-A stimulates ECM deposition by cultured CFs, tissue-specific ablation or bone marrow transplantation would be required to unequivocally pinpoint whether MRTF-A activity primarily occurs in resident cardiac fibroblasts or may also function in additional cell types.

ROCK inhibitors and therapy for pathological fibrosis

Angiotensin converting enzyme (ACE) inhibitors and Angiotensin receptor blockers are among the most effective therapies aimed at preventing cardiac remodeling and congestive heart failure after MI 53. The Rho-ROCK signaling pathway has begun to attract attention as a potential therapeutic target in the treatment of various pathological conditions, including vasospasm, arteriosclerosis, ischemia/reperfusion injury, and renal disease, among others 32, 33, 35, 54. In clinical studies, the ROCK inhibitor, fasudil, has shown efficacy for the treatment of vasospasm and hypertension 55⁻57. Our findings demonstrate the involvement of MRTF-A as a potential transcriptional mediator of TGFβ-1, AngII and ROCK signaling

during fibrotic remodeling following MI. Importantly, MRTF-A$^{-/-}$ mice do not display cardiac rupture or increased post-MI lethality, implying they initially form sufficient scar tissue to undergo wound healing. It is possible that MRTF-A plays a specific role in the promotion of interstitial fibrosis and adverse cardiac remodeling. Characterizing the precise mechanism of MRTF-A activation will enhance our understanding of fibrotic pathologies, and hasten the development of MRTF-A inhibitors that may prove useful for the treatment of fibrotic or cardiovascular disease, circumventing the obvious limitations of general Rho inhibitors, which greatly alter cytoskeletal dynamics.

Novelty and Significance

What is known?

- Following injury cardiac fibroblasts give rise to myofibroblasts, which contribute to scar formation and pathological fibrosis.
- Smooth muscle contractile genes and collagens are highly expressed by the activated myofibroblast after myocardial infarction (MI).
- Myocardin related transcription factor (MRTF) – A is activated by cardiac stress and is a potent inducer of smooth muscle genes.

What new information does this article contribute?

- MRTF-A induces a myofibroblast-like phenotype in cultured cardiac fibroblasts.
- MRTF-A promotes the induction and secretion of collagens by cardiac fibroblasts.
- Mice lacking MRTF-A have a diminished fibrotic response following cardiac injury.

Myocardial infarction arising from coronary artery occlusion is a leading cause of mortality and morbidity in the Westernized world. Damaged cardiac muscle and adjacent healthy myocardium is replaced by scar tissue, which acts as a barrier to re-vascularization, increases susceptibility to arrhythmias, and contributes to progressive cardiac dilatation and loss of contractile function. Understanding the molecular basis of cardiac fibrosis may promote the development of novel therapies for the prevention and treatment of heart failure. Here we demonstrate that MRTF-A controls the expression of a smooth muscle and fibrotic gene program in cardiac fibroblasts, thereby promoting a myofibroblast phenotype. Deletion of MRTF-A in mice results in diminished myofibroblast activation and a dramatic reduction of fibrosis following MI. The protection afforded by MRTF-A deletion is associated with lower expression levels of fibrosis-associated genes, including collagen1a2, a novel direct transcriptional target of MRTF-A. These findings implicate MRTF-A as a key mediator of pathological fibrosis and a potential target for therapeutic intervention for the treatment of cardiovascular disease.

Supplementary Material

Refer to Web version on PubMed Central for supplementary material.

Acknowledgments

We thank Jose Cabrera for graphics and Jennifer Brown for editorial assistance.

Sources of Funding

Work in the lab of E.N.O. was supported by grants from the National Institutes of Health, the Donald W. Reynolds Center for Clinical Cardiovascular Research, The Robert A. Welch Foundation, the American Heart Association and the Jon Holden DeHaan Foundation. E.M.S. was supported by an NIH postdoctoral fellowship. R.D.G was supported by a grant from the NIH.

Non standard abbreviations and acronyms

SRF	serum response factor
MRTF	myocardin related transcription factor
ROCK	Rho-kinase
TGF-β1	transforming growth factor β1
AngII	Angiotensin II
SMA	smooth muscle α-actin
Col 1	collagen type I
AAR	area at risk
ECM	extracellular matrix
MI	myocardial infarction
BZ	border zone
ANF	atrial natriuretic factor
CMC	cardiac myocyte
CF	cardiac fibroblast
LV	left ventricle
RV	right ventricle

References

1. Swynghedauw B. Molecular mechanisms of myocardial remodeling. Physiol Rev. 1999; 79:215–262. [PubMed: 9922372]
2. Tomasek JJ, Gabbiani G, Hinz B, Chaponnier C, Brown RA. Myofibroblasts and mechano-regulation of connective tissue remodelling. Nat Rev Mol Cell Biol. 2002; 3:349–363. [PubMed: 11988769]
3. Serini G, Gabbiani G. Mechanisms of myofibroblast activity and phenotypic modulation. Exp Cell Res. 1999; 250:273–283. [PubMed: 10413583]
4. Wang J, Chen H, Seth A, McCulloch CA. Mechanical force regulation of myofibroblast differentiation in cardiac fibroblasts. Am J Physiol Heart Circ Physiol. 2003; 285:H1871–1881. [PubMed: 12842814]
5. Hinz B. Formation and function of the myofibroblast during tissue repair. J Invest Dermatol. 2007; 127:526–537. [PubMed: 17299435]
6. Eyden B. The myofibroblast: phenotypic characterization as a prerequisite to understanding its functions in translational medicine. J Cell Mol Med. 2008; 12:22–37. [PubMed: 18182061]
7. Cleutjens JP, Verluyten MJ, Smiths JF, Daemen MJ. Collagen remodeling after myocardial infarction in the rat heart. Am J Pathol. 1995; 147:325–338. [PubMed: 7639329]
8. Pipes GC, Creemers EE, Olson EN. The myocardin family of transcriptional coactivators: versatile regulators of cell growth, migration, and myogenesis. Genes Dev. 2006; 20:1545–1556. [PubMed: 16778073]
9. Miano JM. Serum response factor: toggling between disparate programs of gene expression. J Mol Cell Cardiol. 2003; 35:577–593. [PubMed: 12788374]

10. Wang D, Chang PS, Wang Z, Sutherland L, Richardson JA, Small E, Krieg PA, Olson EN. Activation of cardiac gene expression by myocardin, a transcriptional cofactor for serum response factor. Cell. 2001; 105:851–862. [PubMed: 11439182]
11. Wang DZ, Li S, Hockemeyer D, Sutherland L, Wang Z, Schratt G, Richardson JA, Nordheim A, Olson EN. Potentiation of serum response factor activity by a family of myocardin-related transcription factors. Proc Natl Acad Sci U S A. 2002; 99:14855–14860. [PubMed: 12397177]
12. Cen B, Selvaraj A, Prywes R. Myocardin/MKL family of SRF coactivators: key regulators of immediate early and muscle specific gene expression. J Cell Biochem. 2004; 93:74–82. [PubMed: 15352164]
13. Wang Z, Wang DZ, Pipes GC, Olson EN. Myocardin is a master regulator of smooth muscle gene expression. Proc Natl Acad Sci U S A. 2003; 100:7129–7134. [PubMed: 12756293]
14. Small EM, Warkman AS, Wang DZ, Sutherland LB, Olson EN, Krieg PA. Myocardin is sufficient and necessary for cardiac gene expression in Xenopus. Development. 2005; 132:987–997. [PubMed: 15673566]
15. Li S, Wang DZ, Wang Z, Richardson JA, Olson EN. The serum response factor coactivator myocardin is required for vascular smooth muscle development. Proc Natl Acad Sci U S A. 2003; 100:9366–9370. [PubMed: 12867591]
16. Du KL, Ip HS, Li J, Chen M, Dandre F, Yu W, Lu MM, Owens GK, Parmacek MS. Myocardin is a critical serum response factor cofactor in the transcriptional program regulating smooth muscle cell differentiation. Mol Cell Biol. 2003; 23:2425–2437. [PubMed: 12640126]
17. Miralles F, Posern G, Zaromytidou AI, Treisman R. Actin dynamics control SRF activity by regulation of its coactivator MAL. Cell. 2003; 113:329–342. [PubMed: 12732141]
18. Oh J, Richardson JA, Olson EN. Requirement of myocardin-related transcription factor-B for remodeling of branchial arch arteries and smooth muscle differentiation. Proc Natl Acad Sci U S A. 2005; 102:15122–15127. [PubMed: 16204380]
19. Li S, Chang S, Qi X, Richardson JA, Olson EN. Requirement of a myocardin-related transcription factor for development of mammary myoepithelial cells. Mol Cell Biol. 2006; 26:5797–5808. [PubMed: 16847332]
20. Guettler S, Vartiainen MK, Miralles F, Larijani B, Treisman R. RPEL motifs link the serum response factor cofactor MAL but not myocardin to Rho signaling via actin binding. Mol Cell Biol. 2008; 28:732–742. [PubMed: 18025109]
21. Kuwahara K, Barrientos T, Pipes GC, Li S, Olson EN. Muscle-specific signaling mechanism that links actin dynamics to serum response factor. Mol Cell Biol. 2005; 25:3173–3181. [PubMed: 15798203]
22. Kuwahara K, Teg Pipes GC, McAnally J, Richardson JA, Hill JA, Bassel-Duby R, Olson EN. Modulation of adverse cardiac remodeling by STARS, a mediator of MEF2 signaling and SRF activity. J Clin Invest. 2007; 117:1324–1334. [PubMed: 17415416]
23. Zhao XH, Laschinger C, Arora P, Szaszi K, Kapus A, McCulloch CA. Force activates smooth muscle alpha-actin promoter activity through the Rho signaling pathway. J Cell Sci. 2007; 120:1801–1809. [PubMed: 17456553]
24. Mack CP, Somlyo AV, Hautmann M, Somlyo AP, Owens GK. Smooth muscle differentiation marker gene expression is regulated by RhoA-mediated actin polymerization. J Biol Chem. 2001; 276:341–347. [PubMed: 11035001]
25. Philippar U, Schratt G, Dieterich C, Muller JM, Galgoczy P, Engel FB, Keating MT, Gertler F, Schule R, Vingron M, Nordheim A. The SRF target gene Fhl2 antagonizes RhoA/MAL-dependent activation of SRF. Mol Cell. 2004; 16:867–880. [PubMed: 15610731]
26. Olson EN, Nordheim A. Linking actin dynamics and gene transcription to drive cellular motile functions. Nat Rev Mol Cell Biol. 11:353–365. [PubMed: 20414257]
27. Akhmetshina A, Dees C, Pileckyte M, Szucs G, Spriewald BM, Zwerina J, Distler O, Schett G, Distler JH. Rho-associated kinases are crucial for myofibroblast differentiation and production of extracellular matrix in scleroderma fibroblasts. Arthritis Rheum. 2008; 58:2553–2564. [PubMed: 18668558]
28. Fan L, Sebe A, Peterfi Z, Masszi A, Thirone AC, Rotstein OD, Nakano H, McCulloch CA, Szaszi K, Mucsi I, Kapus A. Cell contact-dependent regulation of epithelial-myofibroblast transition via

the rho-rho kinase-phospho-myosin pathway. Mol Biol Cell. 2007; 18:1083–1097. [PubMed: 17215519]

29. Fu P, Liu F, Su S, Wang W, Huang XR, Entman ML, Schwartz RJ, Wei L, Lan HY. Signaling mechanism of renal fibrosis in unilateral ureteral obstructive kidney disease in ROCK1 knockout mice. J Am Soc Nephrol. 2006; 17:3105–3114. [PubMed: 17005937]
30. Fukushima M, Nakamuta M, Kohjima M, Kotoh K, Enjoji M, Kobayashi N, Nawata H. Fasudil hydrochloride hydrate, a Rho-kinase (ROCK) inhibitor, suppresses collagen production and enhances collagenase activity in hepatic stellate cells. Liver Int. 2005; 25:829–838. [PubMed: 15998434]
31. Rikitake Y, Oyama N, Wang CY, Noma K, Satoh M, Kim HH, Liao JK. Decreased perivascular fibrosis but not cardiac hypertrophy in ROCK1+/−haploinsufficient mice. Circulation. 2005; 112:2959–2965. [PubMed: 16260635]
32. Hamid SA, Bower HS, Baxter GF. Rho kinase activation plays a major role as a mediator of irreversible injury in reperfused myocardium. Am J Physiol Heart Circ Physiol. 2007; 292:H2598–2606. [PubMed: 17220176]
33. Hattori T, Shimokawa H, Higashi M, Hiroki J, Mukai Y, Tsutsui H, Kaibuchi K, Takeshita A. Long-term inhibition of Rho-kinase suppresses left ventricular remodeling after myocardial infarction in mice. Circulation. 2004; 109:2234–2239. [PubMed: 15096457]
34. Zhang YM, Bo J, Taffet GE, Chang J, Shi J, Reddy AK, Michael LH, Schneider MD, Entman ML, Schwartz RJ. Targeted deletion of ROCK1 protects the heart against pressure overload by inhibiting reactive fibrosis. FASEB J. 2006; 20:916–925. [PubMed: 16675849]
35. Haudek SB, Gupta D, Dewald O, Schwartz RJ, Wei L, Trial J, Entman ML. Rho kinase-1 mediates cardiac fibrosis by regulating fibroblast precursor cell differentiation. Cardiovasc Res. 2009; 83:511–518. [PubMed: 19406912]
36. Elberg G, Chen L, Elberg D, Chan MD, Logan CJ, Turman MA. MKL1 mediates TGF-beta1-induced alpha-smooth muscle actin expression in human renal epithelial cells. Am J Physiol Renal Physiol. 2008; 294:F1116–1128. [PubMed: 18337547]
37. Qiu P, Feng XH, Li L. Interaction of Smad3 and SRF-associated complex mediates TGF-beta1 signals to regulate SM22 transcription during myofibroblast differentiation. J Mol Cell Cardiol. 2003; 35:1407–1420. [PubMed: 14654367]
38. Qiu P, Ritchie RP, Fu Z, Cao D, Cumming J, Miano JM, Wang DZ, Li HJ, Li L. Myocardin enhances Smad3-mediated transforming growth factor-beta1 signaling in a CArG box-independent manner: Smad-binding element is an important cis element for SM22alpha transcription in vivo. Circ Res. 2005; 97:983–991. [PubMed: 16224064]
39. Morita T, Mayanagi T, Sobue K. Dual roles of myocardin-related transcription factors in epithelial mesenchymal transition via slug induction and actin remodeling. J Cell Biol. 2007; 179:1027–1042. [PubMed: 18056415]
40. Tang RH, Zheng XL, Callis TE, Stansfield WE, He J, Baldwin AS, Wang DZ, Selzman CH. Myocardin inhibits cellular proliferation by inhibiting NF-kappaB(p65)-dependent cell cycle progression. Proc Natl Acad Sci U S A. 2008; 105:3362–3367. [PubMed: 18296632]
41. Poncelet AC, Schnaper HW. Sp1 and Smad proteins cooperate to mediate transforming growth factor-beta 1-induced alpha 2(I) collagen expression in human glomerular mesangial cells. J Biol Chem. 2001; 276:6983–6992. [PubMed: 11114293]
42. Ruteshouser EC, de Crombrugghe B. Characterization of two distinct positive cis-acting elements in the mouse alpha 1 (III) collagen promoter. J Biol Chem. 1989; 264:13736–13739. [PubMed: 2474535]
43. Hendrix JA, Wamhoff BR, McDonald OG, Sinha S, Yoshida T, Owens GK. 5′ CArG degeneracy in smooth muscle alpha-actin is required for injury-induced gene suppression in vivo. J Clin Invest. 2005; 115:418–427. [PubMed: 15690088]
44. Subramanian SV, Polikandriotis JA, Kelm RJ Jr, David JJ, Orosz CG, Strauch AR. Induction of vascular smooth muscle alpha-actin gene transcription in transforming growth factor beta1-activated myofibroblasts mediated by dynamic interplay between the Pur repressor proteins and Sp1/Smad coactivators. Mol Biol Cell. 2004; 15:4532–4543. [PubMed: 15282343]

45. Walker GA, Masters KS, Shah DN, Anseth KS, Leinwand LA. Valvular myofibroblast activation by transforming growth factor-beta: implications for pathological extracellular matrix remodeling in heart valve disease. Circ Res. 2004; 95:253–260. [PubMed: 15217906]
46. van Rooij E, Olson EN. Searching for miR-acles in cardiac fibrosis. Circ Res. 2009; 104:138–140. [PubMed: 19179664]
47. Bujak M, Frangogiannis NG. The role of TGF-beta signaling in myocardial infarction and cardiac remodeling. Cardiovasc Res. 2007; 74:184–195. [PubMed: 17109837]
48. Hao J, Ju H, Zhao S, Junaid A, Scammell-La Fleur T, Dixon IM. Elevation of expression of Smads 2, 3, and 4, decorin and TGF-beta in the chronic phase of myocardial infarct scar healing. J Mol Cell Cardiol. 1999; 31:667–678. [PubMed: 10198196]
49. Bujak M, Ren G, Kweon HJ, Dobaczewski M, Reddy A, Taffet G, Wang XF, Frangogiannis NG. Essential role of Smad3 in infarct healing and in the pathogenesis of cardiac remodeling. Circulation. 2007; 116:2127–2138. [PubMed: 17967775]
50. Yang KL, Chang WT, Hung KC, Li EI, Chuang CC. Inhibition of transforming growth factor-beta-induced liver fibrosis by a retinoic acid derivative via the suppression of Col 1A2 promoter activity. Biochem Biophys Res Commun. 2008; 373:219–223. [PubMed: 18558083]
51. Castano AP, Lin S-L, Surowy T, Nowlin BT, Turlapati SA, Patel T, Singh A, Li S, Lupher ML, Duffield JS. Serum Amyloid P Inhibits Fibrosis Through FcgR-Dependent Monocyte-Macrophage Regulation in Vivo [published online ahead of print November 4, 2009]. Sci Transl Med. 2009 10.1126.scitranslmed.3000111.
52. Haudek SB, Xia Y, Huebener P, Lee JM, Carlson S, Crawford JR, Pilling D, Gomer RH, Trial J, Frangogiannis NG, Entman ML. Bone marrow-derived fibroblast precursors mediate ischemic cardiomyopathy in mice. Proc Natl Acad Sci U S A. 2006; 103:18284–18289. [PubMed: 17114286]
53. Yusuf S, Sleight P, Pogue J, Bosch J, Davies R, Dagenais G. Effects of an angiotensin-converting-enzyme inhibitor, ramipril, on cardiovascular events in high-risk patients. The Heart Outcomes Prevention Evaluation Study Investigators. N Engl J Med. 2000; 342:145–153. [PubMed: 10639539]
54. Satoh S, Ikegaki I, Toshima Y, Watanabe A, Asano T, Shimokawa H. Effects of Rho-kinase inhibitor on vasopressin-induced chronic myocardial damage in rats. Life Sci. 2002; 72:103–112. [PubMed: 12409149]
55. Masumoto A, Mohri M, Shimokawa H, Urakami L, Usui M, Takeshita A. Suppression of coronary artery spasm by the Rho-kinase inhibitor fasudil in patients with vasospastic angina. Circulation. 2002; 105:1545–1547. [PubMed: 11927519]
56. Fukumoto Y, Matoba T, Ito A, Tanaka H, Kishi T, Hayashidani S, Abe K, Takeshita A, Shimokawa H. Acute vasodilator effects of a Rho-kinase inhibitor, fasudil, in patients with severe pulmonary hypertension. Heart. 2005; 91:391–392. [PubMed: 15710736]
57. Kishi T, Hirooka Y, Masumoto A, Ito K, Kimura Y, Inokuchi K, Tagawa T, Shimokawa H, Takeshita A, Sunagawa K. Rho-kinase inhibitor improves increased vascular resistance and impaired vasodilation of the forearm in patients with heart failure. Circulation. 2005; 111:2741–2747. [PubMed: 15927989]

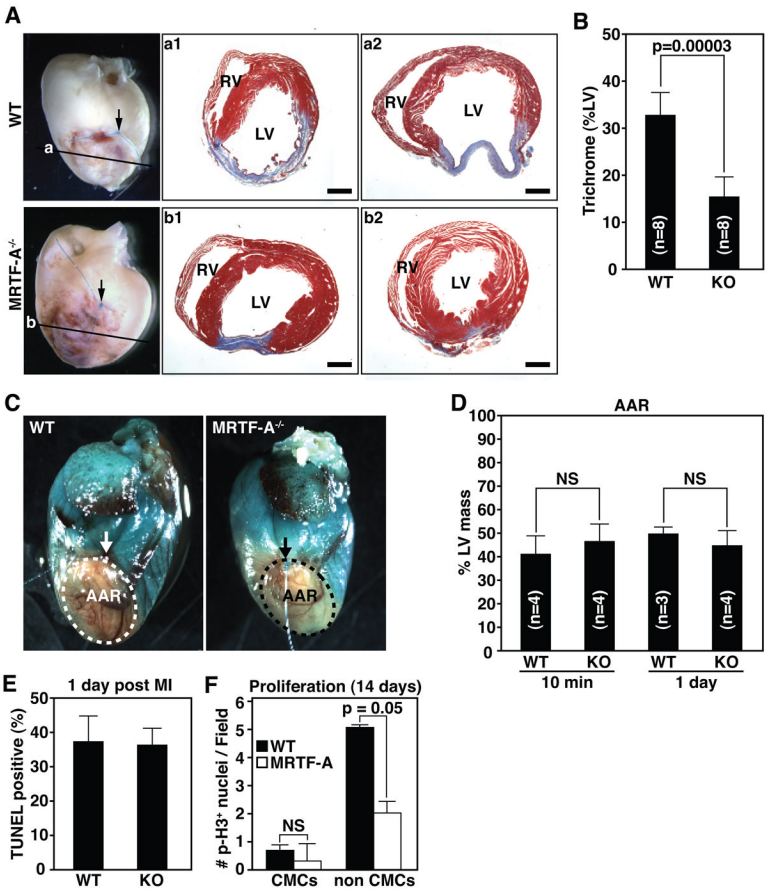

Figure 1. MRTF-A deletion results in reduced scar formation following MI

(A) Whole-mount images of representative hearts 14 days post-MI and Masson's trichrome staining of sections from two representative hearts. Arrow denotes point of ligature and plane of section is illustrated by horizontal line. Masson's trichrome staining illustrates reduced and more compact region of scarring in the infarct zone (compare a1 and a2 to b1 and b2) RV, right ventricle; LV, left ventricle. Scale bar = 1 mm.

(B) Quantification of infarct size presented as the percent LV area positively stained with Masson's trichrome. n=8 WT and 8 KO animals.

(C) Area at risk (AAR) determined by perfusion with methylene blue. AAR is devoid of staining. Arrow denotes point of ligature on the LAD.

(D) Quantification of AAR presented as percent of LV mass that is not stained 10 minutes and 1-day post-MI. n=4 WT and 4 MRTF-A$^{-/-}$ animals at 10 min and 3 WT and 3 MRTF-A$^{-/-}$ animals 1-day post-MI.

(E) Quantification of TUNEL positive cells 1 day post-MI was performed on at least 4 independent fields within the infarct zone of each heart and averaged from 2 WT and 3 MRTF-A$^{-/-}$ animals. Data is represented as percentage of Dapi stained nuclei positive for TUNEL.

(F) Quantification of phospho-histone H3 postive cells 14 days post-MI was performed on at least 7 independent fields in the BZ from each heart and averaged from 3 WT and 4 MRTF-A$^{-/-}$ animals. Error bars indicate the SEM.

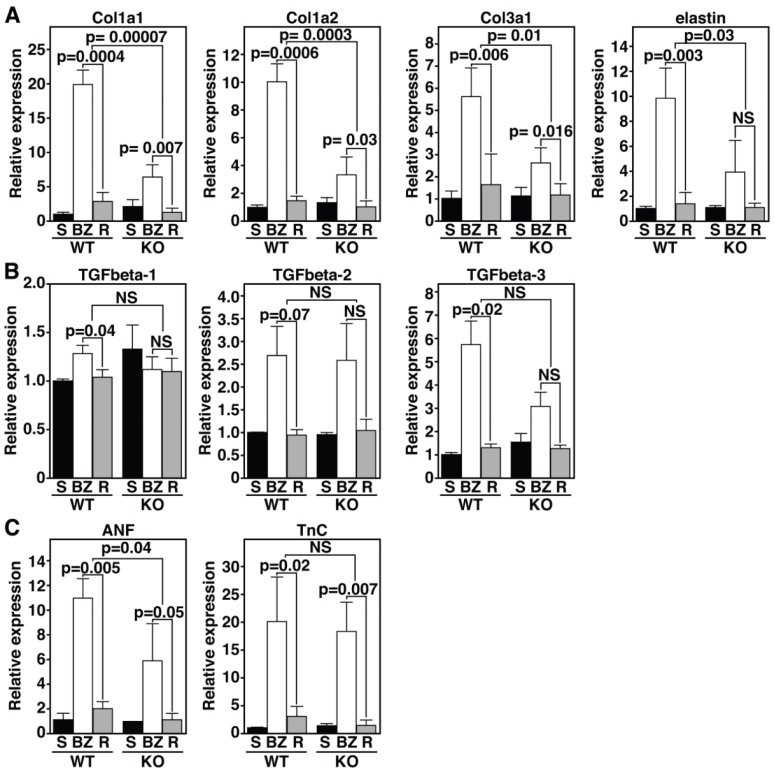

Figure 2. MRTF-A influences ECM gene expression 14 days post-MI

(A) Real time PCR for various ECM components in sham hearts (S) and the border zone (BZ) or remote (R) region of the infarct reveals attenuated expression of collagen genes in the BZ of MRTF-A$^{-/-}$ hearts.

(B) The cytokines TGFβ-1, -2, and -3 do not display significant alterations in expression in the BZ between WT and MRTF-A$^{-/-}$ hearts.

(C) The stress responsive ANF gene displays reduced expression in MRTF-A$^{-/-}$ hearts. TnC levels are elevated to similar levels in the BZ of both WT and MRTF-A$^{-/-}$ animals. n=4 WT and 4 MRTF-A$^{-/-}$ hearts for infarct groups and 2 shams. Error bars represent the SEM.

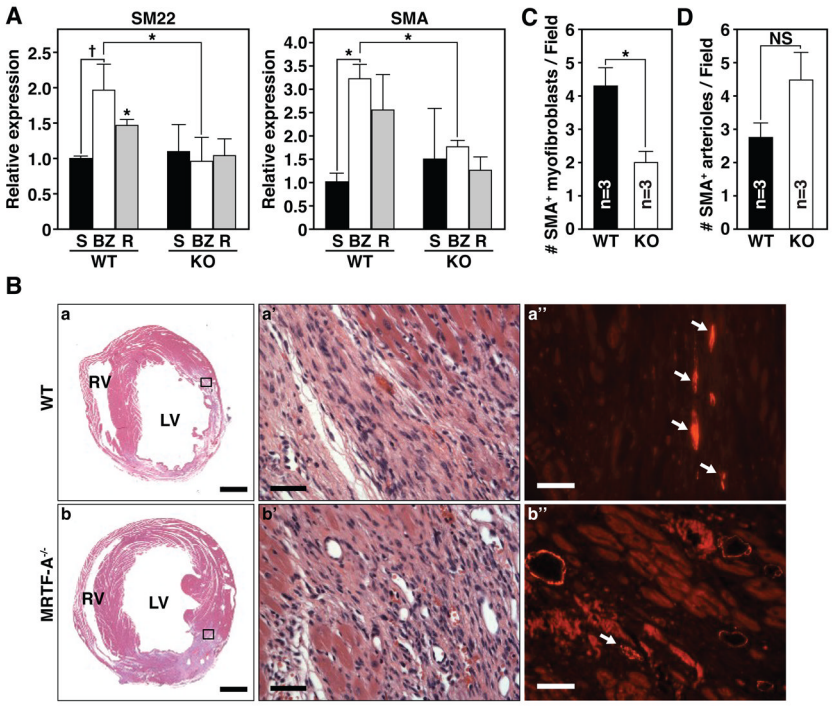

Figure 3. MRTF-A deletion results in altered smooth muscle gene expression 14 days post-MI

(A) Real time PCR reveals a significant reduction of SM22 and SMA induction in both the BZ and remote region of MRTF-A$^{-/-}$ hearts (* denotes p-value < 0.01, and † denotes p-value < 0.05). n=4 WT and 4 MRTF-A$^{-/-}$ hearts per infarct group and 2 shams.

(B) Histological sections of hearts from WT and MRTF-A$^{-/-}$ mice, 14 days post-MI are shown. H&E stained (a, b) sections of representative hearts adjacent to those used for immunohistochemistry illustrate ischemic damage and highlight the BZ of the infarct. (a' and b') Magnification of region that is boxed in a and b. (a" and b") SMA immunostaining corresponding to the boxed region of representative WT and MRTF-A$^{-/-}$ infarcted hearts. Arrows mark SMA-positive spindle-shaped myofibroblasts. Scale bar for a, b = 1mm. Scale bar for a', a" and b', b" = 40 μm.

(C) Number of SMA-positive myofibroblasts per field of view.

(D) Number of SMA positive arterioles in the BZ per field of view. n=3 WT and 3 MRTF-A$^{-/-}$ hearts. Error bars represent the SEM. Quantification was performed at 40x magnification on at least 3 fields of view within the BZ of each heart and averaged from 3 WT and 3 MRTF-A$^{-/-}$ hearts (* denotes p-value < 0.05). Error bars represent the SEM.

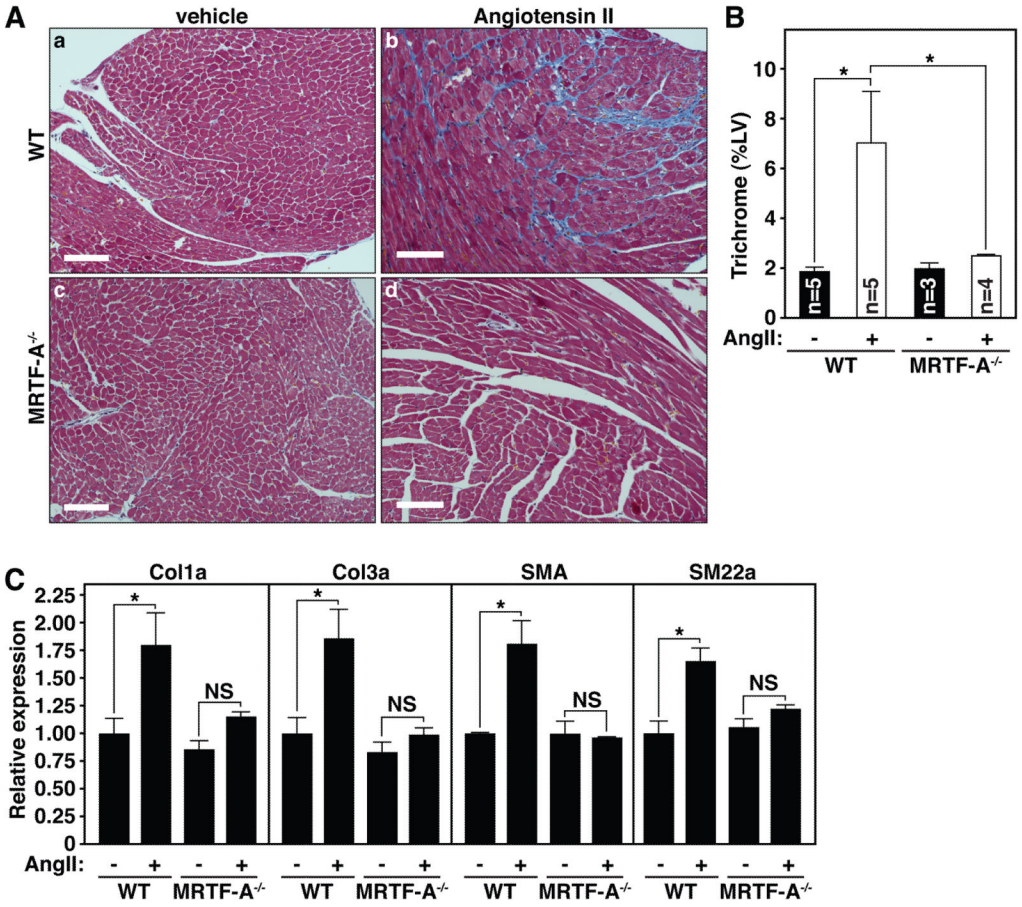

Figure 4. MRTF-A deletion attenuates fibrosis following chronic AngII administration

(A) Masson's trichrome staining of representative histological sections following 14 days of vehicle (a, c) or AngII (b, d) administration in WT (a, b) or MRTF-A$^{-/-}$ (c, d) mice.

(B) Quantification of trichrome staining of the left ventricle (LV). Error bars represent SEM (* denotes p-value < 0.05).

(C) Quantitative RT-PCR for collagen genes and smooth muscle differentiation markers reveals attenuated induction of Col1a, Col3a, SMA and SM22 following AngII administration of MRTF-A$^{-/-}$ animals. Error bars represent SEM (* denotes p-value < 0.05).

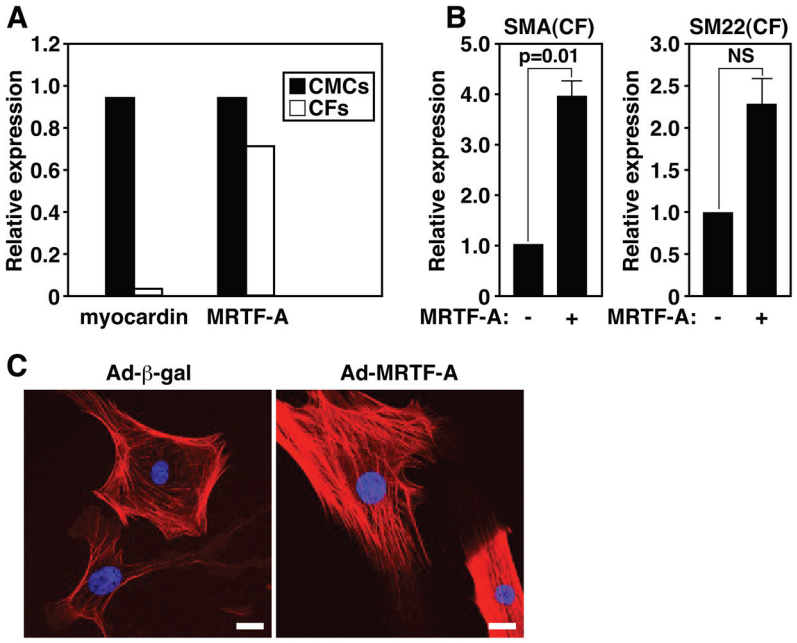

Figure 5. MRTF-A regulates the expression of smooth muscle markers in CFs

(A) Quantitative Real Time PCR reveals myocardin is exclusively expressed in CMCs, while MRTF-A is present in both CMCs and CFs at similar levels.

(B) Quantitative Real Time RT-PCR reveals SMA and SM22 are significantly enriched in CFs over-expressing MRTF-A relative to β-gal infected control CFs. Error bars represent the SEM.

(C) Indirect immunofluorescence of CFs demonstrates MRTF-A over-expression results in the enrichment of SMA into organized stress fibers as compared with Ad-β-gal infected CFs, which display primarily cortical actin SMA staining. Scale bar = 25 μm.

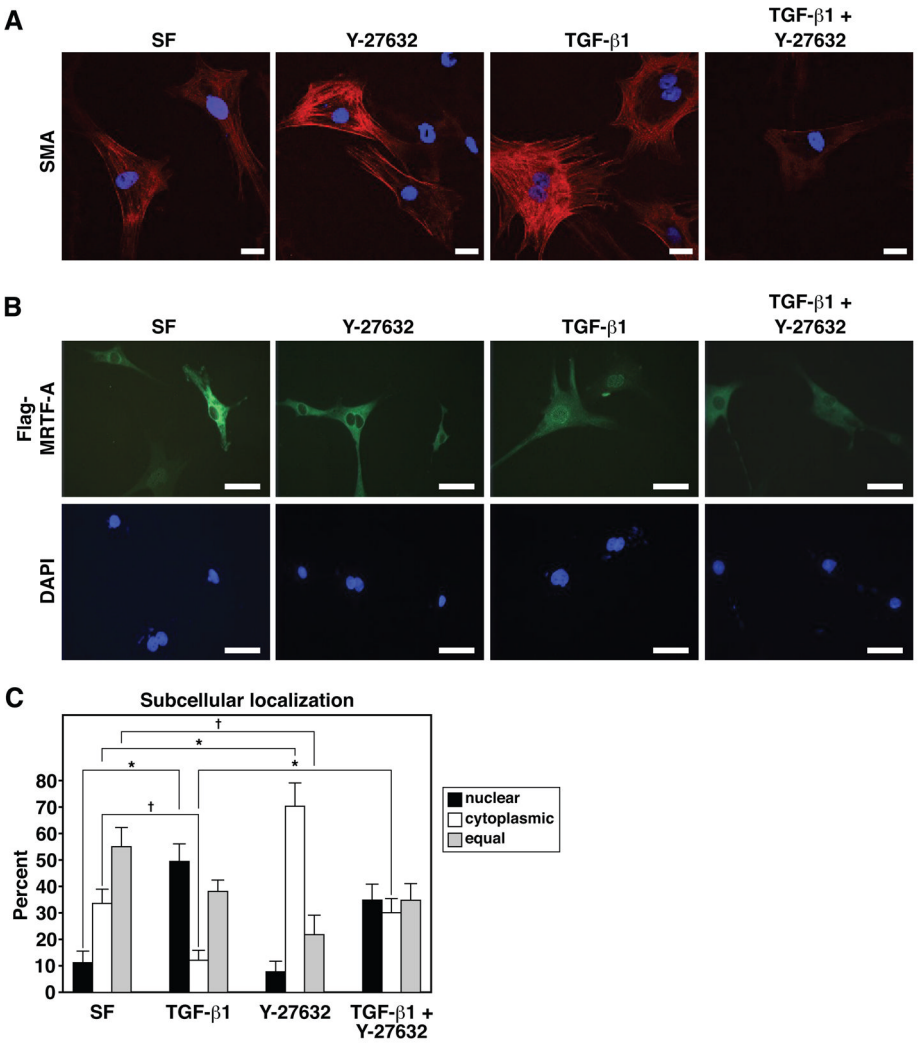

Figure 6. Regulation of MRTF-A nuclear localization and activity in CFs by TGFβ-1 and the ROCK inhibitor, Y-27632

(A) Immunocytochemistry for SMA in CFs grown in serum free (SF) media or media supplemented with TGFβ-1 (10ng/ml), Y-27632 (10μM) or both TGFβ-1 and Y-27632. All images were captured using identical exposure settings. Scale bar = 25 μm.

(B) Immunocytochemical detection of Flag-tagged MRTF-A in CFs after 24 hours of growth in SF media or media supplemented with TGFβ-1, Y-27632 or both TGFβ-1 and Y-27632. Scale bar = 100 μm.

(C) Quantification of the subcellular localization of Flag-MRTF-A under various culture conditions. Subcellular localization of Flag-MRTF-A was scored for approximately 20 random fields of view for each condition. Error bars represent the SEM (* denotes p-value < 0.01; † denotes p-value < 0.05).

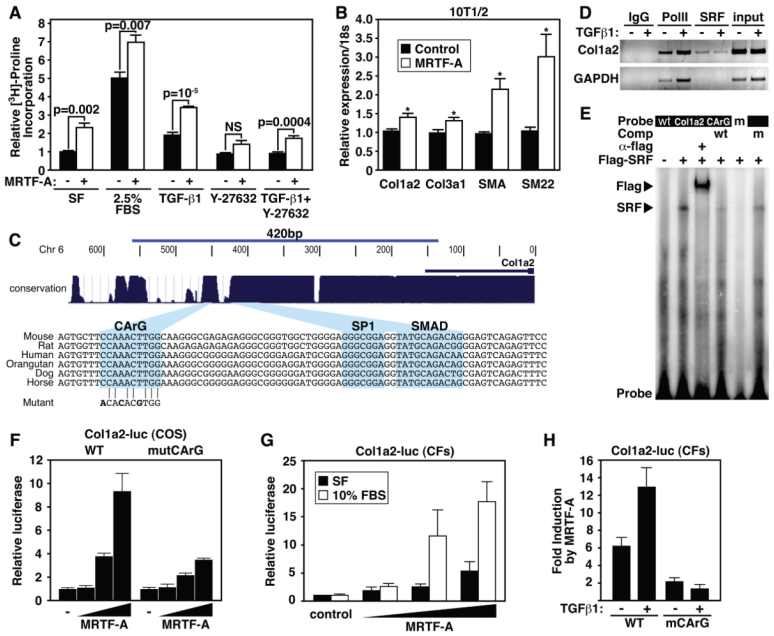

Figure 7. MRTF-A regulates Col1a2 expression

(A) [^{3}H]-proline incorporation in CFs demonstrates MRTF-A significantly enriches collagen synthesis. CFs were serum starved for 48 hrs and then infected with 10 MOI Ad-MRTF-A or Ad-β-gal and cultured in SF media or media supplemented with 2.5% FBS, TGFβ-1 (10 ng/ml), Y-27632 (10 μM), or both TGFβ-1 and Y-27632 for an additional 48 hrs. Error bars represent SEM.

(B) Quantitative Real Time RT-PCR demonstrating the expression of Col1a2, Col3a1, SMA and SM22 in 10T1/2 cells transfected with empty vector control, or MRTF-A expression vector.

(C) Depiction of the region used in transient transfection assays and EMSAs are shown. Blue peaks denote evolutionary conservation and alignment of mammalian regulatory sequences are at bottom highlighting the conserved CArG, SP1 and Smad sites. CArG mutation used in EMSA and transient transfection assays is aligned with WT CArG.

(D) Chromatin immunoprecipitation of Col1a2 or GAPDH promoter sequences with an antibody directed against endogenous SRF. Antibodies directed against PolII or IgG serve as positive and negative controls. Input is 1% of total chromatin.

(E) Electrophoretic mobility assay demonstrates that SRF binds to the conserved CArG box. Flag antibody supershifts the SRF/DNA complex, while WT unlabeled competitor oligonucleotide abolishes the shifted complex. Mutant oligonucleotide (m) fails to bind SRF and unlabeled mutant competitor (m) fails to abolish SRF/CArG interaction.

(F) Transient transfection of COS cells with a WT or CArG mutant Col1a2-luciferase construct reveals dose-dependent responsiveness to MRTF-A. Error bars represent the SD.

(G) MRTF-A induces the expression of Col1a2-luc in transiently transfected CFs and displays increased activity in the presence of 10% FBS. Error bars represent the SD.

(H) MRTF-A dependent Col1a2 promoter activity is stimulated by TGFβ-1 treatment. Mutation of the CArG box abrogates responsiveness of the promoter to MRTF-A or TGFβ-1 treatment. Error bars represent the SD.

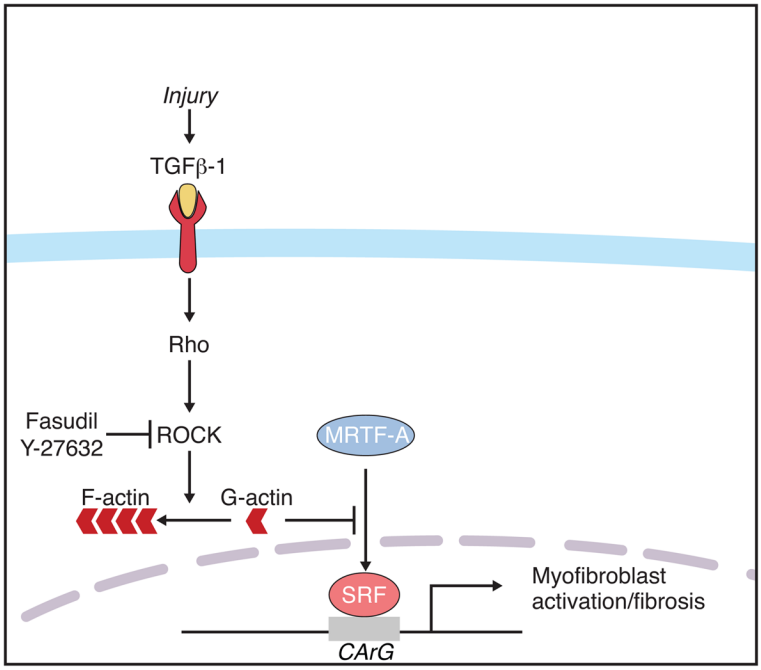

Figure 8. Proposed mechanism of MRTF-A activity during the stress response to MI

Increased TGFβ-1 levels result in the nuclear accumulation of MRTF-A in a Rho-ROCK dependent manner. Nuclear MRTF-A targets CArG box containing genes and induces the expression of smooth muscle and ECM molecules indicative of a myofibroblast cell type.